ELSEVIER

Nuclear Instruments and Methods in Physics Research A 492 (2002) 387–401

NUCLEAR INSTRUMENTS & METHODS IN PHYSICS RESEARCH Section A

www.elsevier.com/locate/nima

Investigation of pixellated HgI_2 γ-ray spectrometers

Zhong He[a,*], Ronald D. Vigil[b]

[a] *Department of Nuclear Engineering and Radiological Sciences, The University of Michigan, Ann Arbor, MI 48109-2104, USA*
[b] *Constellation Technology Corporation, 7887 Bryan Dairy Road, Suite 100, Largo, FL 33777, USA*

Received 2 July 2001; received in revised form 9 May 2002; accepted 18 May 2002

Abstract

HgI_2 gamma-ray spectrometers having small pixel anodes and a thickness of 4–5 mm have been investigated. An energy resolution of 2.9% FWHM was obtained on a 4 mm thick detector using the three-dimensional position sensitive single polarity charge sensing technique. Typical phenomena observed on two detectors are reported and their characteristics are discussed. The results indicate that it is possible to construct efficient gamma-ray spectrometers using commercially available HgI_2 materials if the three-dimensional position sensitive single polarity charge sensing method is implemented.

PACS: 07.85.Nc; 07.85.−m; 07.85.Yk; 29.40.wk

Keywords: HgI_2; Gamma-ray spectrometers; Single polarity charge sensing; Position sensitive detectors; Wide band-gap semiconductors

1. Introduction

HgI_2 has attracted considerable attention since the early 1970s [1] as a potential efficient spectrometer for X- and gamma-rays. This material has a wide band-gap energy of 2.13 eV allowing room-temperature operation, high atomic numbers (80–53) and high density (6.4 g/cm^3) that lead to greater gamma-ray absorption efficiency than other semiconductor detectors. However, some limitations of HgI_2 have restricted its application. These include low mobilities of electrons and holes, significant charge trapping, space charge polarization, material non-uniformity and surface degradation. Although extensive efforts have been invested, the applications of HgI_2 in X- and gamma-ray spectroscopy have been limited mainly to detectors with thickness of 1–2 mm [2–6]. The use of thicker HgI_2 detectors has been very limited [7,8] due to poor energy resolution.

In order to reduce the effects of charge trapping, various pulse processing techniques have been implemented to restore pulse amplitude and to improve energy resolution [6,9]. However, if the drift length of holes during the charge collection time is small compared to the detector thickness, it is impossible to fully recover energy resolution using any pulse processing technique [10]. In 1994, a single polarity charge sensing technique using coplanar grid anodes was implemented on

*Corresponding author. Tel.: +1-734-764-7130; fax: +1-734-763-4540.
E-mail address: hezhong@umich.edu (Z. He).

0168-9002/02/$ - see front matter
PII: S0168-9002(02)01127-0

CdZnTe semiconductor detectors [11], in order to overcome the problem of severe hole trapping which is common in wide band-gap semiconductor detectors. Since the output signal of a device using a single polarity charge sensing method depends on the collection of only one type of charge carriers (electrons on the anode surface), the incomplete charge collection due to trapping of holes in a conventional detector using planar electrodes can be eliminated. Consequently, the energy resolution of CdZnTe detectors with thickness up to 1 cm has been improved dramatically [12–14]. The success of single polarity charge sensing techniques in CdZnTe detectors naturally raises the possibility of similar improvements by applying the same techniques in HgI_2. An attempt was made by Patt et al. [15] in 1995. Anode structures similar to that of a silicon drift detector were fabricated on 2 mm thick HgI_2 detectors, as well as a coplanar grid electrode. Significant improvement in energy resolution was demonstrated for both drift and coplanar grid electrodes. Notably, an energy resolution of 0.9% FWHM at 662 keV gamma-ray energy was obtained on a small circular drift anode. However, it is unclear just how much of the detector volume contributed to the photopeak in these measurements (the peak-to-total ratio is quite low). Also, one could ask whether it is reasonable to expect electrons to travel 5–8 mm (the detector area was $> 2.5\ cm^2$) from the periphery of the circular detector to the central anode with less than 1% electron trapping using a relatively low drift field.

Beginning in 1997 [16], we have studied single polarity charge sensing techniques in HgI_2 detectors produced at Constellation Technologies. Our investigation began by implementing the coplanar grid technique on HgI_2 detectors having a thickness of 4–6 mm. Results from one of the detectors (#V07001), which has an area of about $1.5 \times 1.5\ cm^2$ and a thickness of 6.5 mm, are shown in Fig. 1. The cathode bias was -1800 V and the coplanar grid bias was $+70$ V. The shaping times on the cathode and the coplanar anode were both 10 μs. The ^{137}Cs source was placed at about 6 cm from the anode surface.

Although the measurement results showed that the coplanar grid technique can improve energy resolution in comparison with the conventional planar readout, the photopeak at 662 keV was still very broad. After extensive diagnostic measurements, it was concluded that two factors contributed most to the degradation of energy resolution. The first factor is incomplete electron collection on the collecting anode. Because some unidentified surface properties, the highest bias achievable between the coplanar anodes was about 90 V, above which surface noise breakdown began. When limited to such a relatively low coplanar anode bias (the cathode bias was

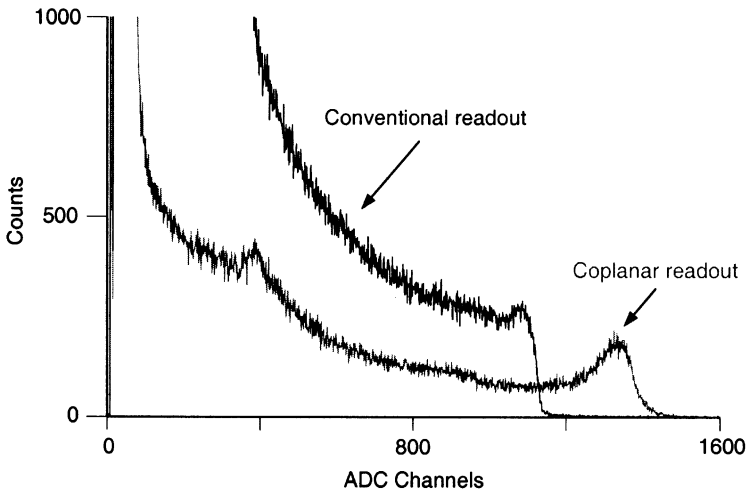

Fig. 1. Energy spectra of ^{137}Cs obtained from a 6.5 mm thick coplanar grid HgI_2 detector.

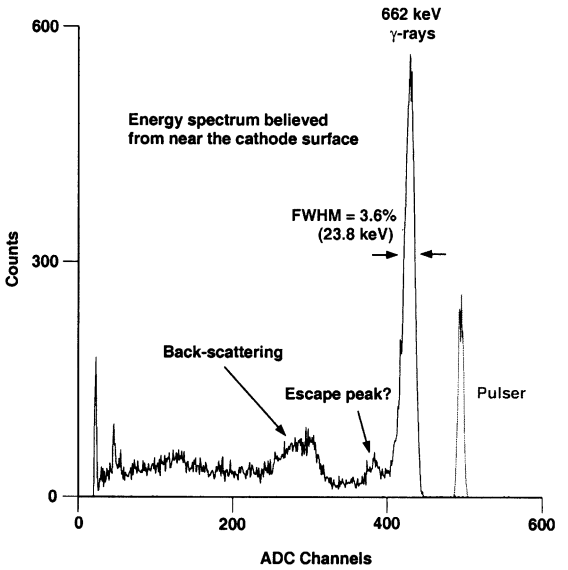

Fig. 2. An energy spectrum of a collimated ^{137}Cs source on a 4 mm thick coplanar grid HgI_2 detector. The events were selected so that the gamma-ray interaction depth was near the cathode.

typically 2000–3000 V), electrons generated by gamma-ray energy deposition may be collected by the non-collecting anode from a significant fraction of events. This phenomenon was confirmed by observing the pulse waveforms at the outputs of preamplifiers on three electrodes (the collecting, the non-collecting anodes and the cathode) simultaneously. If all electrons arrive at the collecting anode and the trapping of electrons is small, the pulse amplitudes from three preamplifiers exhibit unique ratios depending on the depth of gamma-ray interaction. For example, if the energy deposition is near the cathode surface, the collecting anode signal should go to the full amplitude while the non-collecting anode is close to zero, and the difference between the collecting and the non-collecting anode signals should be similar to the cathode signal amplitude ([19], Fig. 2). If the energy deposition is near the anode surface, the collecting and the non-collecting anode signals should have similar amplitude but opposite polarity, and the cathode signal has a very small pulse amplitude. It was observed that the ratios of preamplifier outputs often vary randomly. One possible cause of this phenomenon is the partial collection of electrons by the non-collecting anode. The fractions of electrons arriving at the collecting and non-collecting anodes can depend on the exact location of gamma-ray energy deposition between the two anodes when the inter-anode bias voltage is too low.

The second factor that degraded energy resolution is the non-uniformity of electron trapping at different lateral locations. This is an intractable problem since even depth-sensing coplanar grid readout technique [13,17] cannot compensate for it. This effect was confirmed by observing the improvement of detector performance when the gamma-ray source was collimated. In this case, the gamma-ray interaction location was restricted to a smaller region, and the contribution of material non-uniformity was reduced.

These conclusions were also supported by the following experiment using a 4 mm thick detector (#JBZ001). First, an energy spectrum of ^{137}Cs gamma-rays interacting near the cathode surface was obtained by selecting signals having a large cathode/anode ratio [13,17]. These events are then further divided based on the ratio signal $A1/(A1 - A2)$, where $A1$ is the collecting anode signal and $A2$ is the non-collecting anode signal [18]. If the sharing of electrons collected by the two anodes varies, or if the trapping of electrons changes for different lateral positions, these effects should be reflected by changes in this ratio signal $(A1/(A1 - A2))$ for events having the same $C/(A1 - A2)$ depth parameter. The measurement results confirmed that the photopeak centroid indeed shifts as a function of $A1/(A1 - A2)$ for each fixed $C/(A1 - A2)$ value.

If events with particular ratio parameters are selected, good energy spectra can be obtained from some regions of the detector. One energy spectrum obtained on a 4 mm thick HgI_2 detector (serial #JBZ001) from near the cathode is shown in Fig. 2, where the ratio values were $C/(A1 - A2) = 19$ [0–20] and $100 \times A1/(A1 - A2) = 131$ [128–137]. The ranges shown in brackets indicate that clear photopeaks were observed if the values of ratio parameters fall within these ranges. The 662 keV gamma-rays were incident in the central region of the cathode side and were collimated using a Pb collimator having 4 cm thickness and a

hole of 2 mm in diameter. The pulse shaping times for both the cathode and the coplanar grid anode signals were 6 μs, and the shaping time for the collecting anode was 5 μs. The cathode bias voltage was 3 kV and the bias between the coplanar anodes was 70 V. When gamma-ray events interacting near the cathode surface are selected, the energy spectrum is dominated by photoelectric interactions. This is because if a gamma-ray deposits its energy at more than one location by Compton scattering, the recorded centroid interaction depth would be more likely to lie away from the cathode and the anode surfaces. The energy spectrum shown in Fig. 2 has a high photopeak-to-Compton ratio due to the combination of this effect and the high cross-section of photoelectric interaction of HgI_2. This high photopeak-to-Compton ratio could help in some applications if the peak-to-Compton ratio determines the sensitivity of a system. The prominent back-scattering feature near the Compton edge and the presence of the K X-ray escape peak support the premise that the interactions occurred near the cathode surface.

Despite the good energy resolution shown in Fig. 2 by selecting certain values of $C/(A1-A2)$ and $A1/(A1-A2)$, clear photopeaks were not obtained for all values of the depth parameter $C/(A1-A2)$ and the collection-trapping parameter $A1/(A1-A2)$. This observation showed that the effects of variation of electron collection and trapping cannot be uniquely determined by only these two parameters when the interaction depth is at an arbitrary position within the detector volume.

The trapping of electrons averaged over the detector area was estimated by observing the change in the photopeak amplitude of coplanar grid anode spectra, and the change of the maximum pulse amplitude of cathode spectra [19,20] while the cathode bias voltage was varied. Experimental results showed that the average trapping of electrons across 4–6 mm of HgI_2 at 2000–3000 V cathode bias can be quite small ($<10\%$) on some detectors, offering hope that the single polarity charge sensing technique can achieve good spectroscopic performance on thick HgI_2 gamma-ray detectors.

With sufficient efforts on studying surface properties and fabricating better anode electrodes, the problem of complete electron collection by the collecting anode should be addressable. However, based on the observed material non-uniformity of currently available HgI_2 crystals, the original coplanar grid technique [11], as well as the depth sensing coplanar grid method [13,17] are not promising because they cannot correct the variation of charge trapping across the detector area. Three-dimensional position-sensitive single polarity charge sensing technique [21] then becomes the superior choice for thick HgI_2 gamma-ray spectrometers. The single polarity charge sensing can overcome the problem of hole trapping, and three-dimensional position sensitivity can correct for spatially dependent electron trapping and can mitigate the effects of material non-uniformity.

In order to test whether this approach could improve spectroscopic performance of HgI_2 detectors, four anode pixels having a dimension of about 1×1 mm, surrounded by a common large anode, were fabricated on the anode surface of each detector. Signals from individual pixel anode were read out using discrete charge sensing preamplifiers. A fully pixellated anode array is planned for future evaluation. The following results are for prototype three-dimensional position sensitive detectors with thickness of about 5 mm.

2. Configuration of prototype detectors

A schematic configuration of the anode electrodes and a side view of each device are shown in Fig. 3. The anode electrodes are Pd evaporated through a shadow mask. The dashed curves underneath each pixel anode illustrate the region across which the movement of charge carriers contributes the majority of the induced signal on the corresponding pixel anode. Since only electrons move towards the anode surface, the induced charge on each pixel anode is determined primarily by the number of electrons collected by the pixel. This signal is nearly independent of the distance traveled by the electron in reaching the near-pixel

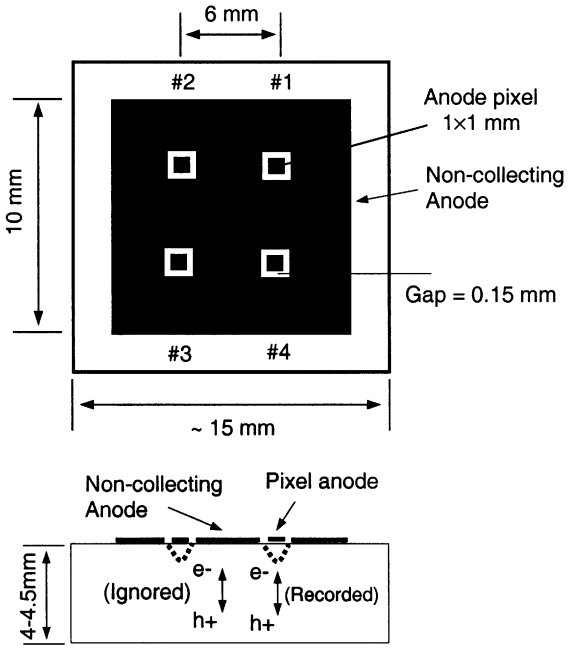

Fig. 3. Schematics of detector configuration. Top: top view of a detector. Bottom: Side view of a detector. The dashed curves near each anode pixel indicate the region across which the movement of electrons contributes ~85% of induced charge on the corresponding pixel anode.

region, and is also nearly immune from the effects of hole motion.

A more detailed calculation of the weighting potential [22] using Coulomb[1] is shown in Fig. 4. It can be seen that about 85% of the induced charge is due to the movement of electrons across ~1 mm distance in the vicinity of the anode surface, and the difference of weighting potentials between different lateral positions underneath the same pixel anode is small (less than a few percent) when the gamma-ray interaction position is 1 mm or further from the anode surface.

3. Stability and pulse waveforms

One of the important properties of any spectrometer is its operational stability. It is well known that HgI_2 detectors may show a polarization effect, especially during the first few days after the initial power-up. During this period, the charge collection characteristics can change with time. On a conventional detector having planar electrodes, since the weighting potential is simply a straight line from 0 to 1 between the cathode and the anode surface [10], the movement of an electron or a hole across a unit distance generates the same amount of induced charge on an electrode. Therefore, the variation of charge transport properties of both electrons and holes over a period of time will contribute equally to changes in the energy spectrum ascribed to the polarization effect. However, in a detector using a single polarity charge sensing technique, the weighting potential changes rapidly near the surface of the anode (if the electron is the collected charge carrier [10]), and much more slowly in the reminder of the detector volume. Therefore, the movement of charge carriers away from the anode surface generates very little induced charge on each pixel anode. This property should significantly reduce the effect of any variations in hole trapping properties over time. Therefore, any changes in energy spectra are mainly determined by changes in electron trapping.

In order to observe the polarization effect in three-dimensional detectors having pixel anodes, spectra of ^{137}Cs gamma-rays were collected over a period of 11 days from anode pixel #3 on a 4.5 mm thick HgI_2 detector (serial #81610R91). The cathode bias voltage was −3000 V. The shaping time for the pixel anode was 6 μs. All anode electrodes were biased at zero voltage. The energy spectra are shown in the top of Fig. 5. A polarization effect was clearly seen during the first 2 days following application of the bias voltage. However, there was no further change in the energy spectrum observed between the 2nd and 11th day (the two spectra overlap very well within statistical fluctuations). It should be noted that the detector had previously been operated with bias voltage prior to the studies reported here. The settling time is usually longer (several days) when a HgI_2 detector is biased for the first time.

Pulse waveforms were also collected from the cathode, the large-area non-collecting anode, and the pixel anode (#3) simultaneously for some

[1] Integrated Engineering Software, 46-1313 Border Place, Winnipeg, Manitoba, Canada R3H OX4.

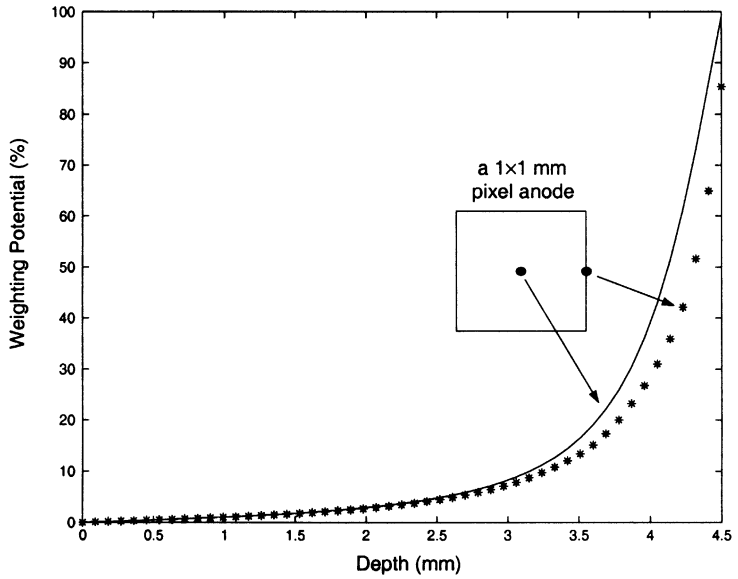

Fig. 4. Calculated weighting potentials of an anode pixel as a function of the distance from the cathode surface. The detector thickness is 4.5 mm. Solid curve: along a perpendicular line directly below the center of the pixel anode. Stars: below the center point of one side as indicated in the figure.

gamma-ray events. For convenience of viewing, the cathode signal is inverted so that it appears to have the same polarity as the signal from the small anode pixel. Pulse waveforms of two typical events, one from near the cathode surface and the other from near the anode surface, are shown in the middle and bottom of Fig. 5. It can be seen that it requires about 1 μs for electrons to drift from the cathode to the anode surface. This gives a mobility for electrons of about 67 cm^2/V s which is lower than the value of ~ 100 cm^2/V s reported in the literature [23,24]. The approximately linear leading edges of the cathode and non-collecting anode signals indicate a relatively uniform electric field within the device, assuming the electron mobility is constant. The rapid rise of pixel anode signal and the rapid fall of the non-collecting anode signal when electrons are approaching the anode surface agree with the calculation of the shape of the weighting potential. These results also show that the pulse amplitude of the cathode signal for the same energy deposition reduces to near-zero when the gamma-ray interaction is located close to the anode. Therefore, the intrinsic signal-to-noise ratio of the cathode signal also becomes small, and therefore no pulse-shaping technique alone can recover the spectroscopic information to the same precision as that achievable for events located near the cathode surface. This observation leads to the conclusion that the energy resolution for a detector using conventional planar electrodes can only be improved at the expense of the detection efficiency by eliminating events that deposit energy close to the anode surface.

4. Detector performance

Several prototype HgI_2 detectors having thickness of 4–4.5 mm have been tested, and some characteristic results are summarized below. In all experiments, charge sensing and amplification on each electrode were performed using standard A250 preamplifiers manufactured by Amptek Inc.,[2] and standard shaping amplifiers (450, 572, 672) from EG&G ORTEC. The signal peak amplitudes of all channels (corresponding to the

[2] Amptek Inc. 6 De Angelo Drive, Bedford, MA 01730, USA.

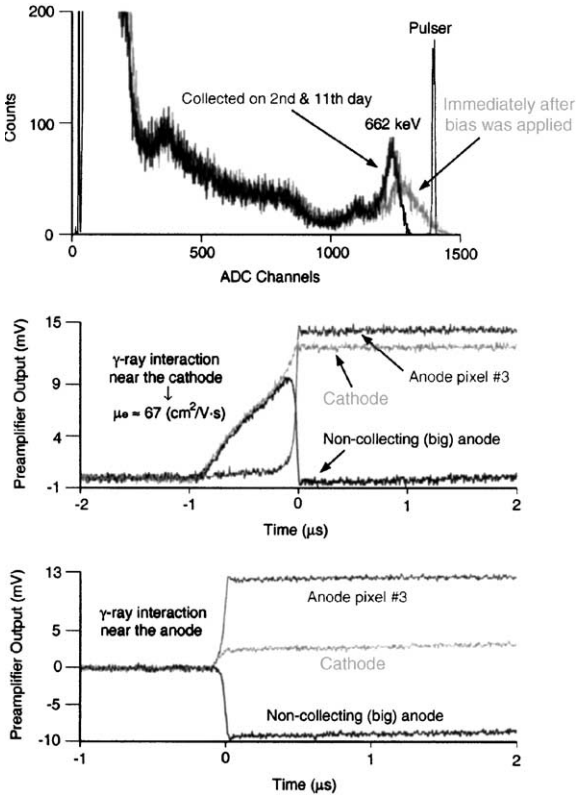

Fig. 5. Stability and pulse waveforms from a 4.5 mm thick HgI_2 detector #81610R91. The energy spectra were obtained from anode pixel #3. Top: Variation of detector performance as a function of time. Middle: Preamplifier output signals for a gamma-ray depositing its energy near the cathode. Bottom: Preamplifier output signals for a gamma-ray depositing its energy near the anode surface.

collecting anode, the non-collecting anode and the cathode) were sampled using a self-made multi-channel peak-hold circuitry. The outputs of the peak-hold electronics were readout by a multi-channel ADC board (RTI-860 manufactured by Analog Devices). The data analysis (to obtain energy spectra for different depth parameters) was performed event-by-event in real time on a PC. The electronic noise of the detector system was measured by injecting test pulses with a fixed amplitude at the input of the preamplifier connected to each pixel anode. The FWHM of each pulser peak is about 0.5% ($\sim$3.5 keV) at 662 keV gamma-ray energy, which can be seen in the top of Fig. 5. This concludes that the broadening of photopeaks (minimum 1.3% FWHM) discussed in following sections is not dominated by the electronic noise of the system.

4.1. Results from a "good" anode pixel

In this experiment, 662 keV gamma-rays (^{137}Cs) were uniformly incident on the cathode surface, and the energy spectra were obtained from anode pixel #3 of a 4.5 mm thick detector (#81610R91). Energy spectra as a function of gamma-ray interaction depth are shown in Fig. 6. The shaping times were 2 and 6 μs on the cathode and the pixel anode, respectively, and the cathode bias was −3000 V. The data collection time was about 83 h in real time. It is evident that clear photopeaks were obtained at all depths underneath this anode pixel. The best energy resolutions of about 1.9% FWHM at 662 keV are from the spectra for gamma-ray interaction depths near the middle of the device, slightly favoring the anode side.

The energy resolution was improved using a shorter shaping time of 1 μs on the anode signal. Three energy spectra are shown in comparison in the top of Fig. 7, corresponding to gamma-rays interacting near the cathode, in the middle between the cathode and the anode, and near the anode, respectively. The photopeak centroid is higher when gamma-rays deposited energy near the mid-plane of the detector. This can be explained as follows: the photopeak amplitude is lower when the interaction location was near the anode side since the change of the weighting potential from

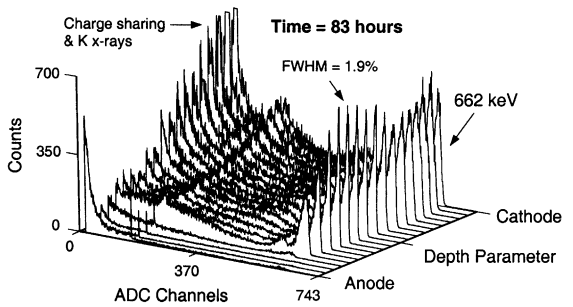

Fig. 6. Energy spectra of ^{137}Cs as function of the depth parameter. Detector #81610R91; anode pixel #3; cathode bias was −3000 V; shaping times were 6 and 2 μs on the anode and cathode signals, respectively.

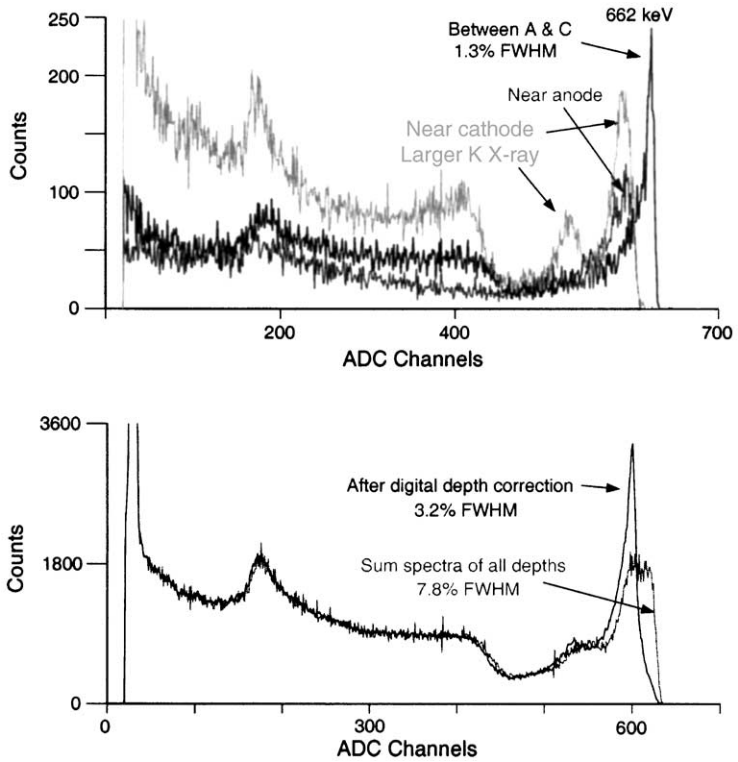

Fig. 7. Top: Energy spectra of ^{137}Cs as a function of the depth parameter when the shaping time was reduced to 1 μs. Bottom: Comparison of energy spectra before and after applying digital depth correction.

the interaction location to the anode surface decreases towards the anode side. Thus the collection of one electron contributes less than one electronic charge to the pixel anode signal. When the interaction position is near the cathode surface, although one collected electron contributes one full electronic charge on the pixel anode, there are fewer electrons collected due to electron trapping. As a result, the maximum photopeak amplitude appears from the events near the midplane of the device. Several energy spectra obtained from this region showed an energy resolution of about 1.3% FWHM. The tail on the lower energy side of each photopeak is expected from charge sharing events, in which a fraction of the electrons are collected by the surrounding non-collecting anode when the gamma-ray interaction position is below the edge of the anode pixel. The sharp decrease on the higher energy side of each photopeak shows the potential of getting better energy resolution. If a fully pixellated anode array can be implemented on the anode surface, these charge sharing events can be identified and processed appropriately. Since photopeak centroids are measured as a function of the depth parameter (cathode/anode), photopeaks can be digitally aligned to form the overall energy spectrum for the corresponding pixel anode. This digital depth correction can correct the variation of photopeak amplitude due to the trapping of electrons and the variation of the weighting potential at different depths. The bottom of Fig. 7 shows the ^{137}Cs energy spectrum obtained by simply adding all spectra from different gamma-ray interaction depths, together with the spectrum resulting from implementation of digital depth correction. The energy resolution was improved from 7.8% to 3.2% FWHM after the depth correction was applied. This comparison demonstrates how the three-dimensional position

sensitive technique corrects the effect of electron trapping for an individual pixel anode.

The average trapping of electrons was obtained by measuring directly the reduction in number of collected electrons at a lower bias voltage [19,20]. The electron mobility-lifetime product can be estimated using

$$(\mu\tau)_e = \frac{D^2}{\ln(N_1/N_2)}\left(\frac{1}{V_2} - \frac{1}{V_1}\right)$$

and the electron mean lifetime using

$$\tau_e = (\mu\tau)_e/\mu_e$$

where N_1 and N_2 are photopeak centroids obtained at cathode bias voltages of V_1 and V_2, respectively. Compared with methods based on the Hecht relation [25], this method is less affected by ballistic deficit and the assumption of uniform electric field within the device. With 59.5 keV gamma-rays (^{241}Am) incident on the cathode side, the photopeak centroids were measured at two cathode bias voltages, -1000 and -3000 V. The shaping time for the pixel anode was 6 μs to ensure good collection of electrons considering the maximum drift time of electrons was about 3 μs at -1000 V cathode bias. The two energy spectra obtained at different bias voltages are shown in Fig. 8. The observed reduction of the photopeak centroid was from 55 to 54 ADC channels when cathode bias was reduced from -3000 to -1000 V, resulting in an electron mobility-lifetime product ($\mu\tau_e$) of about 7.4×10^{-3} cm^2/V. Using the mobility value of $\mu_e = 67$ cm^2/V s, the electron mean lifetime (τ_e) is estimated at about 110 μs which is in agreement with observations by Beyerle et al. on thicker detectors (1 cm thick) [24]. The lower limit of the electron $\mu\tau$ product can be estimated by assuming that the photopeak centroid was reduced at most to 53.5 ADC channels at the cathode bias of -1000 V. This gives an electron mobility-lifetime product ($\mu\tau_e$) greater than 4.9×10^{-3} cm^2/V and the electron lifetime must be greater than 73 μs. There is some evidence that electrons may undergo multiple trapping–detrapping processes while they move towards the anode. More detailed analysis are underway. This long electron lifetime is very promising for the application of single polarity charge sensing techniques in HgI_2.

4.2. Observation from a pixel anode with significant electron trapping

Energy spectra of ^{137}Cs at different depths obtained from pixel #2 of the same detector (#81610R91) discussed in Section 4.1 are shown

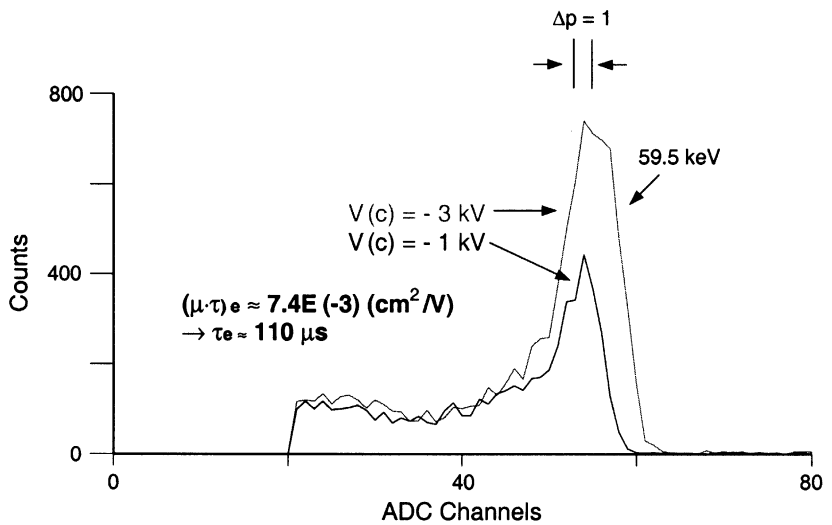

Fig. 8. Comparison of energy spectra obtained from the pixel anode #3 of the first detector at 1 and 3 kV cathode biases. The reduction of the photopeak centroid at lower bias voltage was used to estimate the electron mean lifetime.

in the top of Fig. 9. The photopeak centroid corresponding to the events interacting near the cathode is about $\frac{2}{3}$ of that near the anode side. This indicates that about $\frac{1}{3}$ of the electrons were trapped during the 1 μs drift from the cathode to the anode, giving an estimated mean life time of electrons of only about 2.5 μs. Although digital depth correction can improve the spectroscopic performance, from no photopeak to a clear photopeak as shown in the bottom of Fig. 9, the energy resolution is rather poor (12.3% FWHM at 662 keV after digital depth correction). Because of the severe electron trapping, the photopeak centroid shifted significantly when the depth parameter changed by 1 unit between 0 and 19. Each depth parameter represents a layer about $\frac{1}{20}$ of the detector thickness, which is about 0.25 mm. By dividing spectra further using a finer depth parameter, the energy resolution could be improved slightly, but no significant improvement should be expected. This observation showed that if some region of a detector have poor electron transport properties, the success of three-dimensional position sensitive single polarity charge sensing technique in these regions will be limited.

4.3. A pixel with localized material non-uniformity

Energy spectra of ^{137}Cs with different depth parameters were also obtained from pixel #2 of another 4 mm thick detector (#81610E91). The photopeak area as a function of the depth parameter is shown in the top of Fig. 10. Instead of having a monotonic transition from the anode side to the cathode side as one would expect if gamma-rays interact uniformly within the bulk of the detector, the observed distribution has a peak near the midplane of the detector (around the

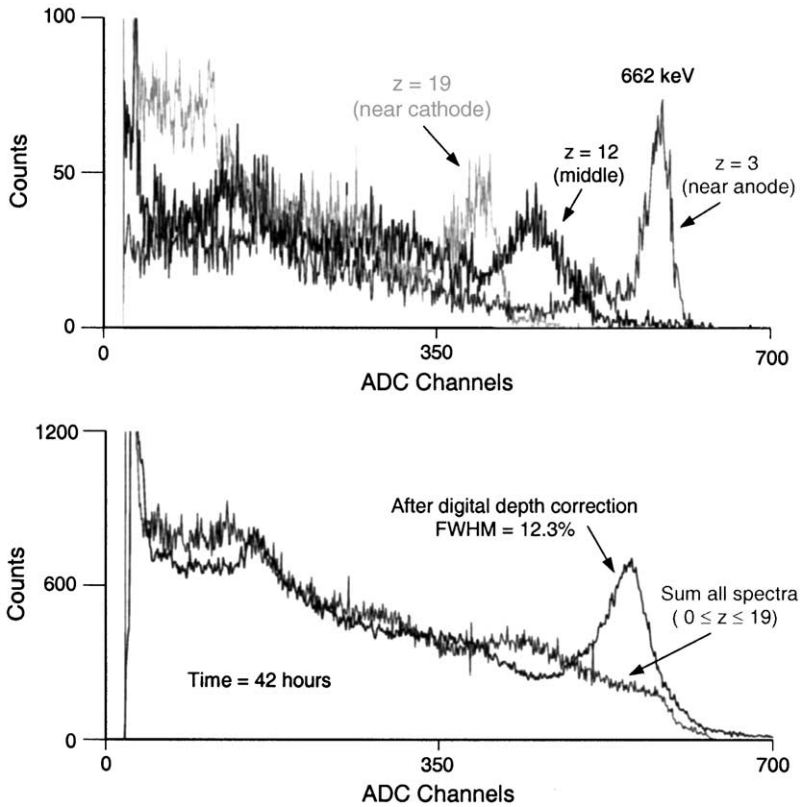

Fig. 9. Top: Energy spectra of ^{137}Cs as function of the depth parameter. A photopeak appears for $1 \leqslant z \leqslant 19$ when depth sensing was applied. Bottom: Comparison of energy spectra before and after applying digital depth correction.

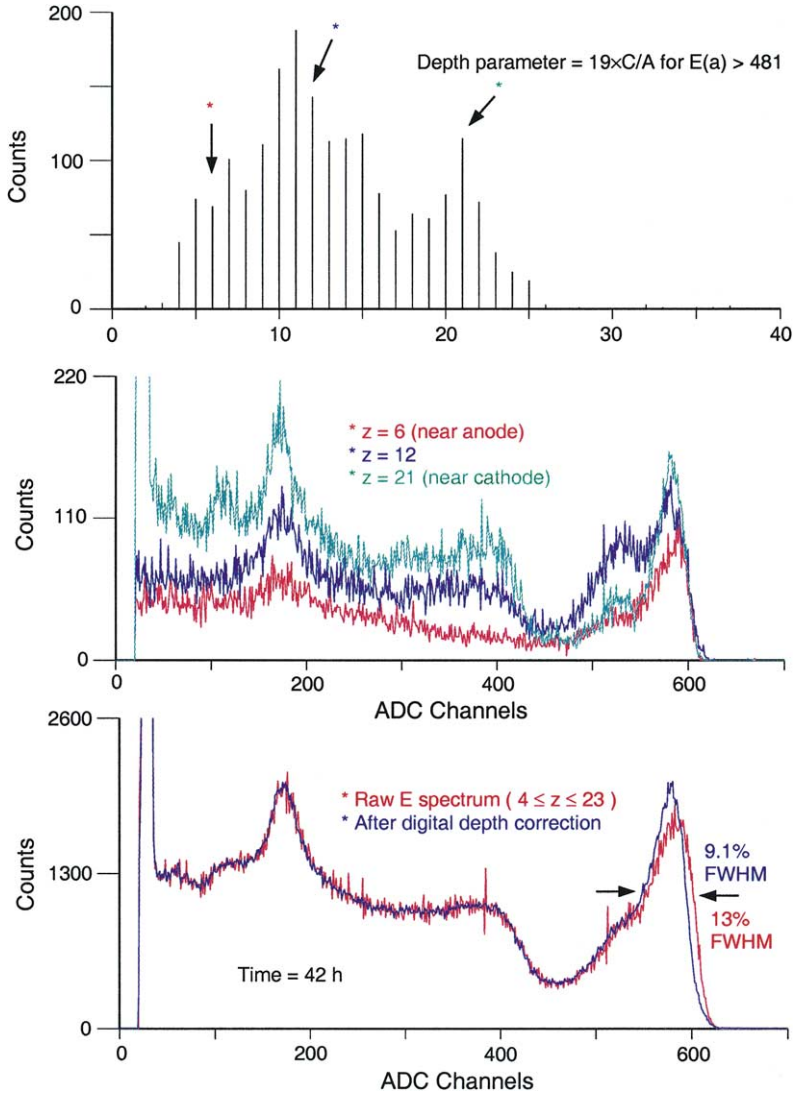

Fig. 10. Top: Photopeak count rate as a function of the depth parameter. Middle: Energy spectra of ^{137}Cs at three depths. Bottom: Comparison of energy spectra before and after applying digital depth correction.

depth parameter of 11). Since the depth parameter is the ratio of the cathode signal and the anode signal, when the trapping of electrons at different lateral positions are different underneath the same pixel anode, the measured depth parameter will be different even for events having the same actual interaction depth. If the electron trapping is higher, the reduction of the pixel anode signal is approximately proportional to the reduction in the number of electrons collected. But the reduction of the cathode signal is less because each trapped electron contributes a fraction of electron charge to the cathode signal before they are trapped. Therefore, the depth parameter would assume a higher value than that corresponding to less electron trapping at the same interaction depth. The specific change of the ratio depth parameter depends on the location and nature of the trapping. If a fixed fraction of electrons is trapped by a grain boundary, the closer the boundary is to

the anode, the greater the depth parameter will appear. The upper limit on the fractional change of the depth parameter is equal to the fraction of electrons trapped by the boundary. This is because when the trapping boundary is very close to the anode, the cathode signal would keep the same amplitude, but the anode pulse amplitude would be reduced by the amount of extra electron trapping at the boundary. This can be understood by

$$z = \frac{\text{Cathode}}{\text{Anode}} \Rightarrow \frac{\Delta z}{z} = \frac{\Delta\text{Anode}}{\text{Anode}}$$
$$\text{when } \Delta(\text{Cathode}) = 0.$$

If the bumps at around 520 ADC channels on the spectra shown in Fig. 10 were due to a trapping boundary in the device, it could explain why all energy spectra have similar structure at the lower energy side of the photopeak if a fixed fraction of electrons was trapped at this boundary. However, this would increase the value of the depth parameter by about 10%, since the photopeak centroids are located near 580 ADC channels ($\Delta(\text{Anode})/\text{Anode} \approx (580 - 520)/580$), for all spectra. Therefore, a trapping boundary is not likely the cause of the observed excessive higher count at a particular depth parameter around 11.

Another possible cause is the non-uniformity of detection volume underneath each anode pixel. If the electric field lines are not straight within the device (perhaps curved due to space-charge distribution or material defects), electrons generated underneath neighboring pixels could also be collected by the central pixel. The variation of photopeak area as a function of the depth parameter could be explained by the variation of effective detection volume underneath the pixel anode, and the common feature on the lower energy side of each photopeak could be due to the charge sharing between neighboring pixels. This assumption can be tested if a fully pixellated anode array is employed on a detector. By observing the uniformity of recorded photopeak events across anode pixels, the effective volume underneath each pixel can be compared and the charge sharing events can be processed accordingly.

The significant difference to the case discussed in Section 4.2 is that the photopeak centroid obtained from different depths are almost the same, which indicate small average electron trapping. However, each photopeak is quite broad. The cause could be the non-uniformity of electron trapping for different microscopic paths underneath the same pixel anode. The improvement in energy resolution using digital depth correction is also limited in this case, when the non-uniformity of electron trapping is significant locally underneath one pixel anode.

4.4. The results from the best pixel anode

Energy spectra of ^{137}Cs obtained from pixel #4 of detector #81610E91 show photopeaks with shapes that are very close to Gaussian. In the top of Fig. 11, three energy spectra are shown for comparison. The first was obtained from the cathode electrode with a shaping time of 6 μs, which is representative of the energy spectrum one would obtain from a conventional detector using planar electrodes. The high-energy cut-off is obvious which corresponds to the case when 662 keV gamma-rays deposit all their energy near the cathode. The spectrum has a continuous transition, with no clear separation between the photopeak and the Compton edge. The other two spectra were from anode pixel #2 and #4, respectively, both with shaping times of 2 μs. Because of the small pixel effect (single polarity charge sensing), photo-peaks from the 662 keV gamma-rays can be clearly seen and are separated from their Compton edges. In addition, the Compton continuum is much flatter than in the cathode spectrum. This is expected from the difference in weighting potentials. For example, if gamma-ray energy is deposited near the mid-plane of the detector, the induced charge on the cathode is only about half of that induced on the anode pixel electrode where the electrons are collected. Therefore, many of the events recorded in the Compton continuum of the cathode spectrum are shifted to higher amplitude in the energy spectra of corresponding pixel anodes. These comparison demonstrate that single polarity charge sensing is superior than conventional read-out using planar electrodes on thick detectors.

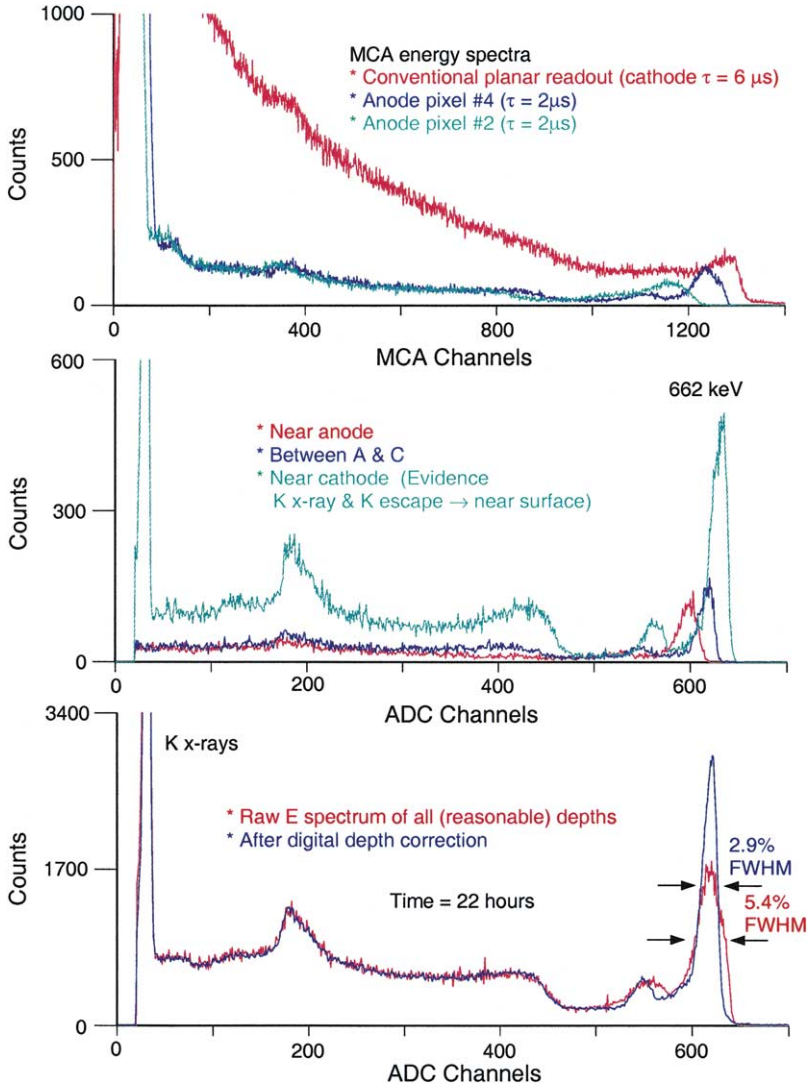

Fig. 11. Top: Comparison of energy spectra using conventional and single polarity charge sensing readouts. Middle: Energy spectra of ^{137}Cs as a function of the depth parameter from pixel anode #4. Bottom: Comparison of energy spectra before and after applying digital depth correction from pixel anode #4.

In the middle of Fig. 11, spectra having different depth parameters are shown for comparison. The photopeak centroid has increasingly higher amplitude when the energy deposition is closer to the cathode. This observation is consistent with the increasing difference of weighting potentials between the value at the anode surface (100% in Fig. 4) and at the position of energy deposition towards the cathode side. It also indicates that the average trapping of electrons during the $\sim$1 μs drift time (see the middle of Fig. 5) is small. Otherwise, the photopeak centroid corresponding to events interacting near the cathode should have a lower amplitude as shown in the top of Fig. 9. When the gamma-ray energy deposition is close to the cathode surface, the K X-ray fluorescence of Hg atoms following a photoelectric interaction has a higher probability of escaping the detector. The

prominent K-shell escape peak can be clearly seen from the energy spectrum for interactions near the cathode surface. By observing energy spectra as a function of the depth parameter, photopeaks only appear in spectra with a measured depth parameter that is smaller than a maximum value, which was 19 in this case. This maximum value of the depth parameter depends on the relative gain between the cathode and the anode pulse processing circuitry, and corresponds to the case when the gamma-ray interaction is near the cathode surface [13,17]. The energy spectra with depth parameter less than 20 were added together to form the overall energy spectrum from all depths underneath pixel anode #4. This spectrum is shown in the bottom of Fig. 11 with an energy resolution of 5.4% FWHM at 662 keV gamma-ray energy. Due to the variation of photopeak centroid with depth, the photopeak is broader than that at a particular depth parameter. This shift of photopeak centroid can be corrected by using digital depth correction, and the corrected spectrum is also shown in comparison in the bottom of Fig. 11. After correction, the energy resolution was improved to 2.9% FWHM and the shape of the photopeak is more nearly a Gaussian distribution. The photopeak-to-Compton ratio was increased by roughly a factor of 2.

By selecting energy spectra having reasonable depth parameters, the energy spectrum can be improved especially at lower energies. Without any discrimination, energy spectra obtained from individual pixel anodes showed very high continuum at low energies. One possibility is that these are charge sharing events when only a small fraction of the electrons are collected by the charge sensing pixel anode. Thus the depth parameter (cathode/anode) should have a much higher value than in the case when electrons are all collected by the anode pixel. By eliminating events with depth parameter higher than the maximum value (19), the K X-rays of Ba at around 35 keV from the ^{137}Cs source were clearly seen from both the spectrum having gamma-ray interaction near the cathode surface and from the overall energy spectrum. The elimination of events having depth parameters higher than 19 does not cause any loss in photopeak efficiency. This procedure discriminates against only the charge-sharing events, which should be correctable if a fully pixellated anode array is employed on the anode surface.

5. Summary and discussions

Two HgI_2 gamma-ray spectrometers with thickness of 4–5 mm have been tested. Each detector has 4 pixellated anode electrodes fabricated in the central region of a large continuous anode so that three-dimensional position-sensitive single polarity charge sensing technique can be studied over a limited portion of the detector volume. Results from 4 pixel anodes with unique characteristics are reported. These results show clearly that the three-dimensional position-sensitive single polarity charge sensing technique is promising for HgI_2 gamma-ray spectrometers with thickness of 4–5 mm, and first results show energy resolution in the range of 2–3% FWHM at 662 keV. However, material non-uniformity of the HgI_2 crystal was also observed. The degree of trapping for electrons can be very different with position even in the same crystal. The average electron trapping can be significant in some regions, and quite small in other parts of the crystal. It was observed that even when the average trapping of electrons is small, the photopeak can still be broad. This effect could due to the variations of charge generation, charge trapping or surface defects altering the electron collection. Investigation of these effects is ongoing.

It should be noticed that digital depth correction was carried out on several spectra shown in Figs. 7, and 9–11. In the digital depth correction technique a different gain is applied to the individual pulses based on their determined depth of interaction, thus calibrating the energy spectra. As a result, the pulse amplitudes corresponding to the same energy deposition are aligned at the same channel in the total corrected spectrum, regardless of the interaction depths. There is no loss of events from this correction method.

One important advantage of three-dimensional position sensing is that energy spectrum can be formed by selecting events which depositing their energy in the better region of the detector material,

even if only a fraction of the crystal shows good charge transport properties. Preferential selection of regions within the crystal volume could result in better energy resolution at the expense of detection efficiency.

Acknowledgements

This work was supported by Pinellas County Industry Council of Florida and Constellation Technology Corporation. We thank Professor Glenn F. Knoll for his interest and support throughout this project, his valuable discussions and comments on our manuscript, Dr. Beverly Haeger for her strong support of this project, Dr. Lodewijk van den Berg for his help with crystal growth, selection and valuable discussions, Vernon Brenda Gerrish for helpful discussions, James Berry for the design of shadow masks, Yanfeng Du for his calculation of weighting potentials, and Juanita Baker for her excellent work on detector fabrication.

References

[1] W.R. Willig, Nucl. Instr. and Meth. 96 (1971) 615.
[2] D. Orthendahl, et al., IEEE Trans. Nucl. Sci. NS-29 (1) (1982) 784.
[3] B.E. Patt, et al., IEEE Trans. Nucl. Sci. NS-33 (1) (1986) 523.
[4] B.E. Patt, et al., Nucl. Instr. and Meth. A 366 (1995) 173.
[5] V. Gerrish, Nucl. Instr. and Meth. A 322 (1992) 402.
[6] G.F. Knoll, Radiation Detection and Measurement, 3rd Edition, Wiley, New York, ISBN 0-471-07338-5, 2000, pp. 484–486.
[7] P. Olmos, et al., Nucl. Instr. and Meth. A 299 (1990) 45.
[8] L. van den Berg, Nucl. Instr. and Meth. A 322 (1992) 453.
[9] A. Beyerle, et al., Nucl. Instr. and Meth. A 242 (1986) 443.
[10] Zhong He, Nucl. Instr. and Meth. A 463 (2001) 250.
[11] P.N. Luke, Appl. Phys. Lett. 65 (1994) 2884.
[12] P.N. Luke, et al., Nucl. Instr. and Meth. A 458 (2001) 319.
[13] Z. He, et al., Nucl. Instr. and Meth. A 388 (1997) 180.
[14] J.M. Perez, Z. He, D.K. Wehe, IEEE Trans. Nucl. Sci. NS-48 (3) (2001) 272.
[15] B.E. Patt, et al., Nucl. Instr. and Meth. A 380 (1996) 276.
[16] Zhong He, Technical Reports 1997–1999, to Constellation Technology Corporation, 7887 Bryan Dairy Road, Suite 100, Largo, Florida 33777, USA.
[17] Z. He, et al., Nucl. Instr. and Meth. A 380 (1996) 228.
[18] Z. He, G.F. Knoll, D.K. Wehe, Y.F. Du, Nucl. Instr. and Meth. A 411 (1998) 107.
[19] Z. He, G.F. Knoll, D.K. Wehe, Nucl. Instr. and Meth. A 411 (1998) 114.
[20] Z. He, G.F. Knoll, D.K. Wehe, J. Appl. Phys. 84 (10) (1998) 5566.
[21] Z. He, et al., Nucl. Instr. and Meth. A 422 (1998) 180.
[22] Y.F. Du, private communications.
[23] R.C. Whited, M.M. Schieber, Nucl. Instr. and Meth. 162 (1979) 113.
[24] A. Beyerle, et al., Proc. MRS 16 (1983) 191.
[25] K. Hecht, Z. Phys. (Germany) 77 (1932) 235.